ELSEVIER

J. Construct. Steel Res. Vol. 36, No. 3, pp. 215–234, 1996

0143-974X/96 $15.00 + 0.00

0143-974X(95)00018-6

Collapse Strength of Rectangular Plates under Transverse Compression

C. Guedes Soares & J. M. Gordo

Unit of Marine Technology and Engineering, Instituto Superior Técnico, Universidade Técnica de Lisboa, Av. Rovisco Pais, 1096 Lisboa, Portugal

(Received 12 July 1994; revised version received 6 April 1995; accepted 25 May 1995)

ABSTRACT

This paper presents a proposal for a new design equation to predict the collapse strength of plates under transverse compression both with restrained and unrestrained boundary conditions. The equation is developed from and calibrated with experimental and numerical results which allows an assessment of the uncertainty involved in its application. Finally, the proposed equation is compared with the predictions of a non-linear finite element code, which was used to verify in a systematic fashion the effect of changing some of the governing parameters.

NOTATION

a	Plate length
b	Plate width
b_e	Effective plate width
B_c	Modelling factor for the strength of unrestrained plates [eqn (17)]
B_y	Modelling factor for transverse strength [eqn (15)]
E	Young's modulus of elasticity
K	Buckling coefficient [eqn (13)]
R_α	Reduction factor for longitudinal strength of a plate with aspect ratio α relative to a square plate strength [eqn (9)]
t	Plate thickness
w	Amplitude of the initial imperfections
α	$= a/b$—Aspect ratio
α_y	$= b/a$—Transverse aspect ratio [eqns (10) and (11)]
β	$= b/t\sqrt{\sigma_0/E}$—Plate slenderness

β_y	$= a/t\sqrt{\sigma_0/E}$—Transverse plate slenderness [eqns (10) and (11)]
σ_x	Longitudinal strength ratio
ϕ_{xa}	Longitudinal strength ratio of a plate with $\alpha < 1$
ϕ_y	Transverse strength ratio
ϕ_{ym}	Strength ratio of the midfield of a plate loaded transversely [eqn (8)]
ϕ_{yp}	Ultimate transverse strength ratio present proposal
ϕ_{yu}	Ultimate transverse strength ratio of unrestrained plates
ν	Poisson's ratio
ψ	Coefficient accounting for nonuniform load distribution [eqn (13)]
σ_{cr}	Critical elastic stress
σ_{ycr}	Critical stress in the transverse direction
σ_e	Buckling stress
σ_{ed}	Edge stress
σ_0	Yield stress
σ_u	Ultimate stress

1 INTRODUCTION

The strength of plates under transverse loading was an important problem several years ago when transverse stiffening was frequently used in ship structures. With the increasing use of longitudinal stiffening in ship structures attention has concentrated more on plates with aspect ratios greater than 1, i.e. on plates loaded in the longitudinal direction. However, in offshore and civil engineering structures, where biaxial loading is present and the transverse loading is not negligible, knowledge of the plate behaviour under transverse loading is important.

When the plate aspect ratio becomes significantly smaller than unity as happen in the transverse compression case, the mode of plate failure becomes different in that the central part of the plate does not feel the restraining effect of the short edges, and behaves like a column. Unlike plates, columns have negligible post-buckling resistance,[1] which indicates that the ultimate stress of plates due to transverse compression would be much less than to longitudinal compression. Therefore, it is important to quantify the strength of plates under transverse loading.

In any consideration of transverse plate strength, the influence of weld-induced residual stresses is expected to be small because the short edges are well away from the centre of the plate. The influence of initial distortions should also be small in this case, due to the presence of modes of distortion in the longitudinal direction of the plate greater than 1 which tend to increase the strength of the plate. These modes correspond to higher critical elastic buckling stresses than the one of a plate with a single half-wave. This increase in strength counteracts the increase in the amplitude of distortions.

The shape of the imperfection that would degrade the plate strength more is in the form of a half-sine wave in the transverse direction. This shape may exist when the plate is subjected only to transverse loading. However, in biaxially loaded plates the simultaneous presence of longitudinal load will tend to induce a higher mode longitudinal deformation pattern with the buckles going up and down alternately, which may even increase the transverse plate strength. This effect is of the same nature of the one related to initial imperfections of mode higher than 1, but snap effects are of different importance.

This work tackles the problem of deriving the design equation by starting with an assessment of the model uncertainty in existing design equations and by developing a new one which has a model uncertainty with a bias close to unity. The model uncertainty is assessed by comparing available experimental and numerical examples with the model predictions, as was performed in ref. 2 for the case of longitudinal strength.

2 EXISTING FORMULATIONS OF TRANSVERSE PLATE STRENGTH UNDER COMPRESSION

For the case of the simply supported plate, Bleich[3] derived one of the earliest explicit expressions for the effective width b_e as a function of edge stress, σ_{ed}:

$$\frac{b_e}{b} = \frac{1+\alpha^4}{1+3\alpha^4} + \frac{2\alpha^4}{1+3\alpha^4}\frac{\sigma_{cr}}{\sigma_{ed}} \quad (1)$$

where $\alpha = a/b$ is the aspect ratio, a is the plate length, b is its width and σ_{cr} is the critical longitudinal buckling stress. Carlsen[4] conducted a numerical study using a finite-difference code and concluded that Bleich's formula was too optimistic for high levels of compression.

One of the earlier formulations of ultimate transverse plate strength is due to Schultz,[5] who presented results from a Galerkin solution of the Von Karman's large deflection plate equations. Another one is due to Blanc,[6] which has even been adopted by some Classification Societies. He based his formulation on the assumption that after plate buckling the two edge strips would be carrying the whole load. Faulkner *et al.*[7] transformed it to an ultimate effective width formula which implies that the edge strips are at the yield stress:

$$\phi_y = \frac{\sigma_u}{\sigma_0} = \frac{0.9}{\beta^2} + \frac{1.9}{\beta\alpha} \cdot \left(1 - \frac{0.9}{\beta^2}\right) \tag{2}$$

where β is the plate slenderness and σ_0 is the yield stress:

$$\beta = \frac{b}{t}\sqrt{\frac{\sigma_0}{E}} \tag{3}$$

which is a function of the breadth b and thickness t of the plate, as well as of the material properties, σ_0 and modulus of elasticity E.

Becker and Colao[8] assumed that the transverse strength of a plate would decrease from the square plate strength as a function of α which they proposed in the form of a multiplication factor γ:

$$\gamma = \frac{1}{(\alpha - 1)^2 + 1}. \tag{4}$$

They proposed a design equation for the transverse compression strength of the plate, which was based on an effective width approach and which was updated by Becker[9] to read:

$$\phi_y = 0.923\left\{\frac{2}{\alpha}\left(\frac{b_e}{b}\right) + \left[1 - \frac{2}{\alpha}\left(\frac{b_e}{b}\right)\right](1 - C)\gamma\frac{\sigma_{ycr}}{\sigma_0} + 0.077\right\}, \tag{5}$$

where C is a degradation coefficient that is zero for a perfect plate and 1 for a plate with imperfections and σ_{ycr} is the transverse elastic critical strength.

Valsgard[10] conducted a series of calculations using a finite-difference code to predict the transverse compression strength of plates with an aspect ratio of 3 and compared them with the predictions of the methods of Blanc–Faulkner and Schultz. He concluded that both formulations over-estimated the real plate strength for stocky plates and under-estimated the strength of slender plates.

Valsgard proposed a new formula for the ultimate strength which is based on a principle similar to Blanc's:

$$\phi_y = \frac{\sigma_u}{\sigma_0} = \frac{\phi_x}{\alpha} + 0.08 \cdot \left(1 + \frac{1}{\beta^2}\right)^2 \cdot \left(1 - \frac{1}{\alpha}\right) \text{ with a maximum of 1.0} \tag{6}$$

where ϕ_x is the uniaxial compression strength of a simply supported square plate according to Faulkner:[11]

$$\phi_x = \frac{2}{\beta} - \frac{1}{\beta^2} \, (\beta \geq 1). \tag{7}$$

The rationale behind his approach is to consider that the plate can be divided into two fields. The first one is adjacent to the transverse edges and due to its proximity to the edges, it is considered to be part of a square plate and thus to have a strength ratio equal to ϕ_x. The middle of the plate constitutes the second zone, whose strength was considered by Blanc to be the buckling strength, but Valsgard fitted it to the results of his numerical calculations leading to:

$$\phi_{ym} = 0.08 \cdot \left(1 + \frac{1}{\beta^2}\right)^2. \tag{8}$$

By varying the aspect ratio, eqn (6) can predict the strength of square plates. In this case, the prediction of the formula should be equal to the uniaxial longitudinal compression strength. However, the numerical results of Valsgard predict too high values of strength in those cases as concluded in the analysis reported hereafter.

The existing formulae of plate transverse compression strength are based on an assumption about the mode of plate failure which is valid for long plates, i.e. for aspect ratios larger than 2. The range of plate dimensions with an aspect ratio between 1 and 2 will not be well represented by those formulae.

The case of a plate in transverse compression with an aspect ratio between 1 and 2 is the same as a longitudinally loaded plate with aspect ratio between 1 and 0.5. This case has been studied by Guedes Soares and Faulkner[12] who derived a model correction factor R_α that reduces the square plate strength predictions to ones applicable to a plate of lower aspect ratio, $\alpha_y = 1/\alpha$, so that:

$$\phi_{x\alpha} = \phi_x R_\alpha \quad \text{for} \quad 1.0 \leq \beta \leq 3.5 \tag{9}$$

where ϕ_x is the square plate strength given by eqn (7) and $\phi_{x\alpha}$ is the longitudinal strength of a plate with aspect ratio α_y or, which is the same, the transverse compression strength of a plate with aspect ratio α.

The strength reduction factor was chosen to be of the form:

$$R_\alpha = 1 + (A - B\beta_y)(1 - \alpha_y) \tag{10}$$

which becomes unity when $\alpha_y = 1$ and decreases with increasing slenderness, as was observed in the data. The longitudinal slenderness of a plate with low aspect ratio is defined as $\beta_y = a/t\sqrt{\sigma_0/E}$. Estimation of the regression coefficients A and B from the data lead to the proposed form of:

$$R_\alpha = 1 + (0.55 - 0.16\beta_y)(1 - \alpha_y) \quad \text{for} \quad 0.5 \le \alpha_y \le 1.0. \tag{11}$$

The critical transverse compression strength of plate elements derived from elastic analysis leads to the Bryan elastic buckling stress. Some codes, like the Rules of the American Bureau of Shipping (ABS), use this critical elastic stress as design stress combined with the Johnson–Ostenfeld formulation to account for the effect of plastic deformations. The critical buckling strength σ_{cr} of a plate is equal to the elastic buckling strength σ_e:

$$\frac{\sigma_{cr}}{\sigma_0} \equiv \frac{\sigma_e}{\sigma_0} = \frac{\pi^2}{12(1-\nu^2)}\frac{K}{\beta^2} \quad \text{for} \quad \sigma_e \le 0.5\sigma_0 \tag{12}$$

when buckling occurs in the elastic range, i.e. $\sigma_e \le 0.5\sigma_0$. Poisson's ratio ν is 0.3 for steel plates and the buckling coefficient K accounts for the type of loading and boundary conditions. According to ABS rules, for a wide plate with linearly varying transverse loading this factor is given by:

$$K = \left(1 + \frac{1}{\alpha^2}\right)\frac{2.1}{\psi + 1.1} \quad \text{for } 0 \le \psi \le 1 \tag{13}$$

where the factor ψ is such that when the stresses on one end of a transverse edge of the plate are σ, they are $\psi \cdot \sigma$ on the other one. Thus, for plates under uniform compressive stresses $\psi = 1$.

When the predicted strength is greater than half the yield stress, the collapse strength is given by:

$$\frac{\sigma_{cr}}{\sigma_0} = 1 - \frac{1}{4}\frac{\sigma_0}{\sigma_e} \quad \text{for } \sigma_e > 0.5\sigma_0 \tag{14}$$

which implies an elasto-plastic collapse.

3 ANALYSIS OF EXISTING RESULTS

There is only a small number of results available for the transverse strength of plate elements.[9,13–16] Becker and co-workers[9,13] presented results of experiments on small tubes of square cross-section. This type of experiment has the drawback of not allowing a very good definition of the boundary conditions at the plate edges, as will become clear in the discussion of the results. Bradfield and Porter Goff[16] tested eight plates with low aspect ratio, but only four of them correspond to transversely loaded plates since the remainder are square plates.

Numerical results are available from Dowling *et al.*[14] and Valsgard.[15] In these cases the boundary conditions are defined precisely and one is able to assess their effect on the plate strength. Restrained conditions correspond to the situation where the in-plane displacements perpendicular to the edge are zero, while in constrained conditions the edge is specified to remain straight, but is free to pull-in. Unrestrained conditions imply that all in-plane displacements are free.

The available experimental results indicate, in general, a strength lower than the predicted values, as can be observed in Table 1, which summarises the results of experiments and numerical predictions of plate transverse compression strength. To provide a common base for the comparisons, both types of results have been normalised by the predictions of eqns (2), (6) and (12).

In the case of the formulation of Blanc and Faulkner [eqn (2)] the average of the normalised experimental results was 0.70, while it was 0.85 for the numerical results, i.e. a difference of *ca* 18%. In the case of Valsgard's formulation [eqn (6)] these values were, respectively, 0.89 and 1.11, a 20% difference. These differences may be due to the presence of weld-induced stresses and initial distortions in the experimental results which are not accounted for explicitly in eqns (2) and (6). This is further supported by the observation that the experimental results show a larger variability than the numerical ones, indicating the influence of fabrication factors and experimental errors.

TABLE 1

Results of 20 Tests and 12 Numerical Results for the Ultimate Transverse Compression Strength of Plates Normalised by Faulkner's Formulation [eqn (2)], Valsgard's Approach [eqn (6)], the Present Proposal (GS,G) [eqn (15)], and the ABS Formulation [eqns (12)–(14)]

References		β	α	*b/t*	*Exper.* ϕ_{exp}	*ABS* ϕ_{exp}/ϕ_y	*Faulk.* ϕ_{exp}/ϕ_y	*Valsg.* ϕ_{exp}/ϕ_y	*GS,G* ϕ_{exp}/ϕ_y
Becker[13]	Average	2.20	3	60	0.30	0.90	0.52	0.76	0.72
	S.D.	0.82	0	22	0.23	0.05	0.15	0.36	0.36
Becker[8]	Average	2.90	3	50	0.22	1.25	0.57	0.72	0.66
	S.D.	1.16	0	20	0.11	0.36	0.06	0.20	0.21
Becker[8]	Average	2.90	1.5	50	0.50	2.12	0.92	1.11	0.93
	S.D.	1.16	0	20	0.14	1.05	0.12	0.03	0.11
Bradfield[16]	Average	1.49	1.63	33	0.74	1.00	0.84	1.04	1.02
	S.D.	0.56	0.58	13	0.16	0.08	0.23	0.16	0.20
All tests	Average	2.19	2.3	45	0.47	1.17	0.70	0.89	0.84
	S.D.	1.09	0.79	21	0.28	0.52	0.23	0.27	0.29
Valsgard[10]	Average	2.18	2.8	55	0.51	1.54	0.85	1.11	1.01
	S.D.	0.97	1.5	25	0.25	0.80	0.22	0.16	0.07

Therefore, it seems more appropriate to use only the numerical results as a basis to calibrate the design formulae, considering also that they allow better control of the boundary conditions. From the available results, the ones of Valsgard[15] represent the most complete and consistent set of data and therefore they were adopted as the reference data against which the presently proposed equation was developed.

Valsgard's design equation [eqn (6)] was the one that showed both a smaller bias and a smaller uncertainty. Thus, it was chosen as the basic equation to be improved.

The present proposal for transverse compression strength was obtained by modifying Valsgard's formulation ϕ_y [eqn (6)] by a model parameter B_y:

$$\phi_{yp} = \phi_y \cdot B_y. \tag{15}$$

The model parameter is represented by:

$$B_y = (a_1\beta + a_2)(a_3\alpha + a_4) \tag{16a}$$

where the a_is are regression coefficients. A regression analysis of the numerical data indicated that:

$$B_y = 0.589 + 0.130\alpha + 0.252\beta - 0.069\alpha\beta. \tag{16b}$$

The performance of eqns (15) and (16) has been checked in the same fashion as eqns (2) and (6), and the results are included in the last columns of Tables 1 and 2. This formula has been calibrated with the numerical results of Valsgard[10] and in that case it had a bias of 1.01 and the standard deviation of the errors was reduced to 7% as compared with the 16% from eqn (6) and 22% from eqn (2).

The ABS strength formulation is based on the Johnson–Ostenfeld approach and the critical elastic strength is represented by eqns (12)–(14). The results in Table 2 indicate that this formulation is conservative by *ca* 33% on average and has a large model uncertainty of 68%. For the experimental tests the formulation is conservative by 17% and for the numerical results by 54% (Table 1). It is clear that the equation gives better results for the experimental tests than for the numerical predictions, although the latter are preferred for calibration. The results are very conservative for β greater than 3.5 (Table 2) and there is a large sensitivity to the aspect ratio. On the other hand, the ABS strength formulation agrees well with the experimental results in the range of slenderness below 2.5. Even for the combined data included in Table 2 it shows good performance for $\beta < 2.5$, which is in fact the important range in several types of structures.

TABLE 2
Tests and Numerical Results of the Ultimate Transverse Compression Strength Sorted by Slenderness

Refer.	β	α	*b/t*	*Measur* ϕ_{exp}	*ABS* ϕ_{exp}/ϕ_y	*Faulk.* ϕ_{exp}/ϕ_y	*Valsg.* ϕ_{exp}/ϕ_y	*GS,G* ϕ_{exp}/ϕ_y
16	0.63	2.5	15	1.00	1.09	1.39	1.00	1.03
16	0.94	1.7	23	0.97	1.11	0.97	1.30	1.39
10	0.99	1.0	25	1.05	1.12	0.98	1.05	1.16
10	0.99	2.0	25	0.68	0.82	0.68	1.02	1.06
10	0.99	3.0	25	0.60	0.76	0.61	1.08	1.05
10	0.99	5.0	25	0.54	0.72	0.57	1.17	1.02
16	0.99	2.5	24	0.77	0.96	0.78	1.29	1.30
	for		Average		0.94	0.85	1.13	1.15
	$\beta < 1$		Stand. Dev.		0.16	0.26	0.12	0.13
13	1.10	3.0	30	0.68	0.93	0.76	1.34	1.30
10	1.58	1.0	40	0.86	1.04	0.76	1.00	0.99
10	1.58	2.0	40	0.49	0.87	0.65	0.95	0.92
10	1.58	3.0	40	0.40	0.88	0.64	1.01	0.96
10	1.58	5.0	40	0.32	0.82	0.62	1.07	0.98
16	1.71	1.7	35	0.55	0.98	0.71	0.99	0.95
16	1.71	1.7	35	0.56	1.00	0.73	1.02	0.98
16	1.72	1.0	38	0.70	0.88	0.65	0.85	0.82
16	1.72	1.0	38	0.74	0.93	0.69	0.90	0.87
8	1.74	1.5	30	0.65	1.08	0.80	1.09	1.04
8	1.74	3.0	30	0.38	1.02	0.68	1.03	0.97
8	1.74	3.0	30	0.32	0.87	0.58	0.88	0.83
8	1.74	3.0	30	0.30	0.81	0.54	0.81	0.77
13	1.84	3.0	50	0.28	0.85	0.54	0.80	0.75
	for		Average		0.93	0.67	0.98	0.94
	$\beta < 2$		Stand. Dev.		0.08	0.08	0.13	0.13
16	2.48	1.0	59	0.62	1.07	0.77	0.96	0.82
13	2.57	3.0	70	0.14	0.84	0.40	0.50	0.46
10	2.63	1.0	67	0.77	1.49	1.02	1.26	1.05
10	2.63	2.0	67	0.41	1.99	0.91	1.13	0.98
10	2.63	3.0	67	0.29	1.80	0.86	1.06	0.96
10	2.63	5.0	67	0.20	1.41	0.78	0.96	0.97

(*continued*)

TABLE 2
(Continued)

Refer.	β	α	*b/t*	*Measur* ϕ_{exp}	*ABS* ϕ_{exp}/ϕ_y	*Faulk.* ϕ_{exp}/ϕ_y	*Valsg.* ϕ_{exp}/ϕ_y	*GS,G* ϕ_{exp}/ϕ_y
	for		Average		1.43	0.79	0.98	0.87
	$\beta < 3$		Stand. Dev.		0.39	0.19	0.23	0.20
13	3.30	3.0	90	0.10	0.96	0.38	0.42	0.37
10	3.51	1.0	89	0.77	2.64	1.35	1.58	1.16
10	3.51	2.0	89	0.38	3.28	1.16	2.29	1.03
10	3.51	3.0	89	0.26	2.87	1.08	1.15	1.02
10	3.51	5.0	89	0.16	2.04	0.93	0.94	1.03
	for		Average		2.36	0.98	1.08	0.92
	$\beta < 4$		Stand. Dev.		0.80	0.33	0.39	0.28
8	4.05	1.5	70	0.36	3.17	1.04	1.14	0.82
8	4.05	3.0	70	0.11	1.66	0.56	0.55	0.48
8	4.05	3.0	70	0.10	1.42	0.48	0.47	0.41
8	4.05	3.0	70	0.12	1.70	0.57	0.57	0.49
	for all β		Average		1.33	0.77	0.99	0.92
			Stand. Dev.		0.68	0.24	0.25	0.24

Figures 1–4 show the different strength curves applicable for plate aspect ratios of 1, 2, 3 and 5. For the lower aspect ratios it is apparent that the proposed equation predicts lower strengths for stocky plates and higher ones for slender plates. However, for large aspect ratios the present proposal approaches Valsgard's, i.e. the model parameter B_y approaches unity.

Another feature that is of interest is the fact that the difference between those formulations and the curve for infinite plate strength is significant for small aspect ratios, but becomes small for an aspect ratio of 5.

Figure 5 shows all the experimental (E) and numerical (N) results independently of the aspect ratio, normalised by the predictions of the present design equation proposal. Apart from two numerical results with a strength around 0.35, which are both from Dowling,[14] most of the numerical results lie close to 1.0. However, the experimental results, in particular the ones of Becker *et al.*,[13] show a strong bias, with values around 1.3 for $\beta \approx 1$ and 0.4 for $\beta \approx 3.5$. This figure illustrates well the fact that those results may be affected by the adoption of the square tubes used in those experiments. This implies rotational restraint, as well as weld-induced stresses at the edges. The low bias at high

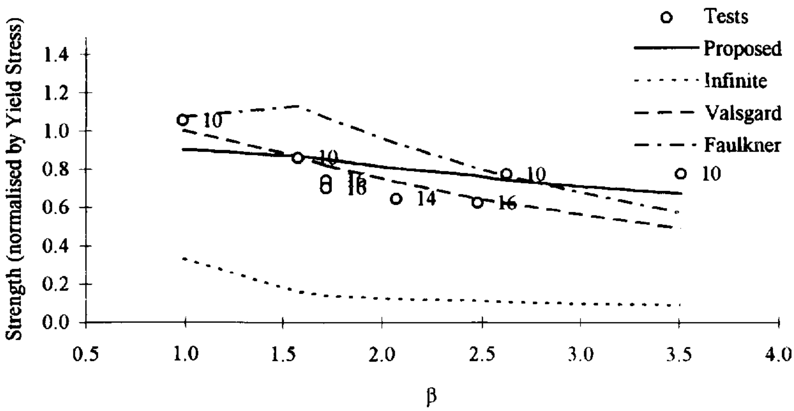

Fig. 1. Transverse compressive strength of plates with $a/b = 1$, as given by different authors. Faulkner's curve represented here is given by eqn (2), but for correct use one should use eqn (7). The labels in the figure indicate the reference from which the data was obtained.

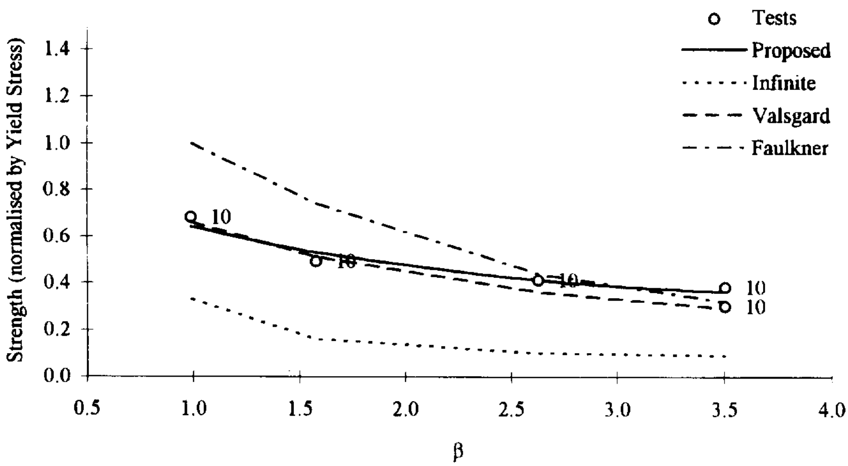

Fig. 2. Transverse compressive strength of plates with $a/b = 2$, as given by different authors. The labels in the figure indicate the reference from which the data was obtained.

slenderness was confirmed by additional experiments[8] for a slenderness near 4 and an aspect ratio of 3 (Figs 3 and 5).

An attempt has been made to include explicitly in the formulation the effect of the weld-induced residual stresses and initial distortions. Much less data is available indicating explicitly the value of these defects. Figures 6 and 7 indicate the strength as a function of those parameters for the cases available. Figure 6 shows a wide spread of results which do not allow any definite conclusion to be drawn. Figure 7 shows, surprisingly, that most results lie around 1.0, irrespective of the value of initial distortions, while one would

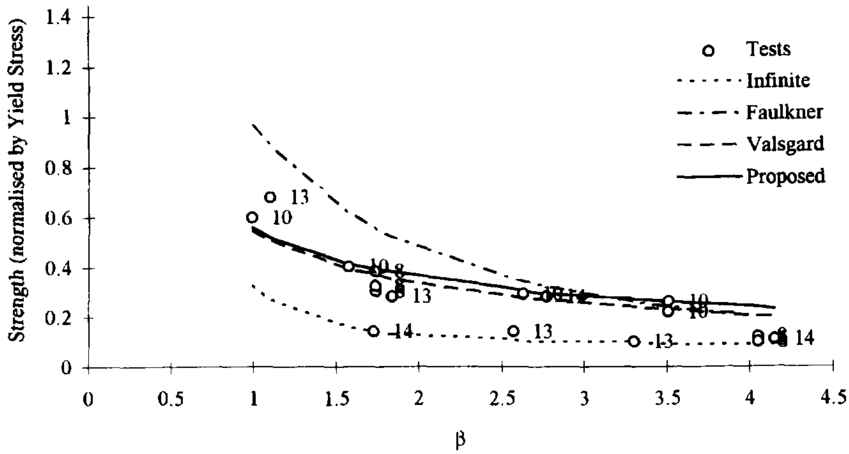

Fig. 3. Transverse compressive strength of plates with $a/b = 3$, as given by different authors. The labels in the figure indicate the reference from which the data was obtained.

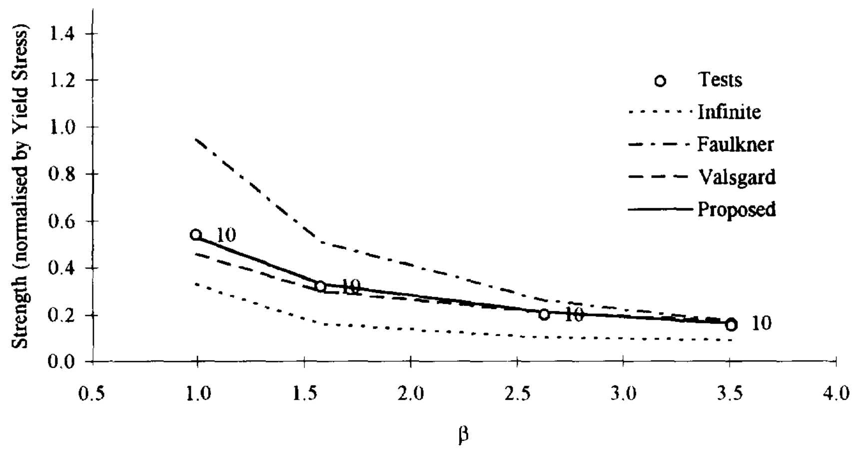

Fig. 4. Transverse compressive strength of plates with $a/b = 5$, as given by different authors. The labels in the figure indicate the reference from which the data was obtained.

expect that, with increasing initial deflections, eqn (15) would be predicting weaker plates. At any rate, the available data does not support the inclusion of an additional parameter in eqn (15) to account explicitly for the effect of residual stresses or of initial distortions.

Rotational restraints along the edges of the plate are generally neglected assuming that anti-symmetric lateral deformations take place in adjacent plate fields. This is valid whenever lateral pressure loads are small.

The analysis of the results indicated in Table 3 shows that the boundary conditions are important in determining the plate strength, especially for aspect

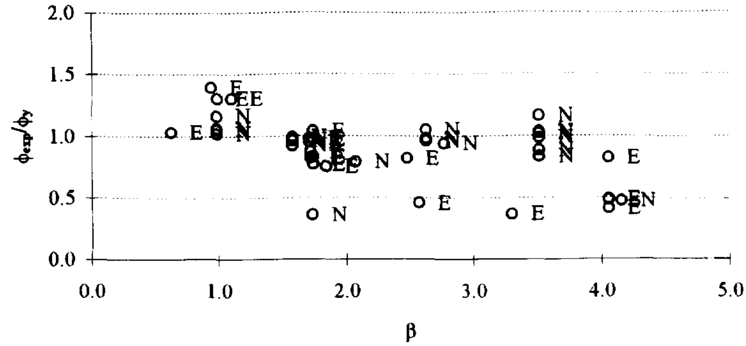

Fig. 5. Experimental (E) and numerical (N) results normalised by the presently proposed design equation.

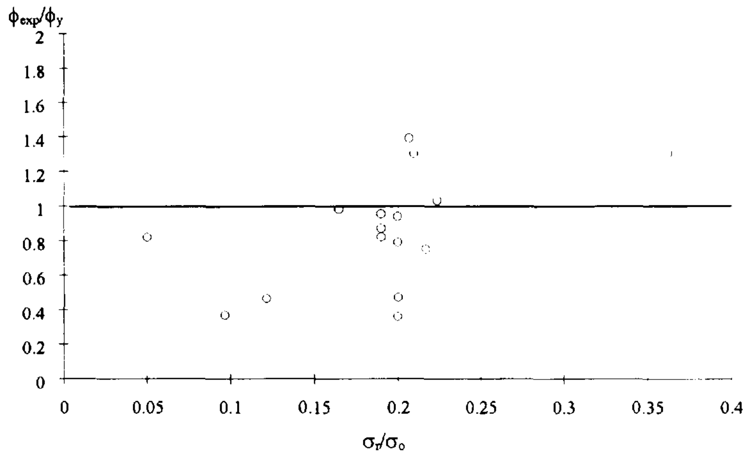

Fig. 6. Strength modelling factor as a function of residual stress level.

ratios smaller than 3. For plates with $\alpha = 2$ changing boundary conditions from restrained to unrestrained can induce strength reductions of *ca* 20%, while this is only 5% for plates with $\alpha = 5$. The importance of modelling the effect of boundary conditions has already been identified by Guedes Soares[2] for the case of uniaxial compression.

Adopting the proposed eqn (15) to predict the transverse compression strength of unrestrained plate elements, it is possible to define another multiplication factor B_c which allows strength predictions for unrestrained plates ϕ_{yu} to be obtained from eqn (15):

$$\phi_{yu} = \phi_y B_c. \tag{17}$$

Using the few results given in Table 3, this factor was defined as:

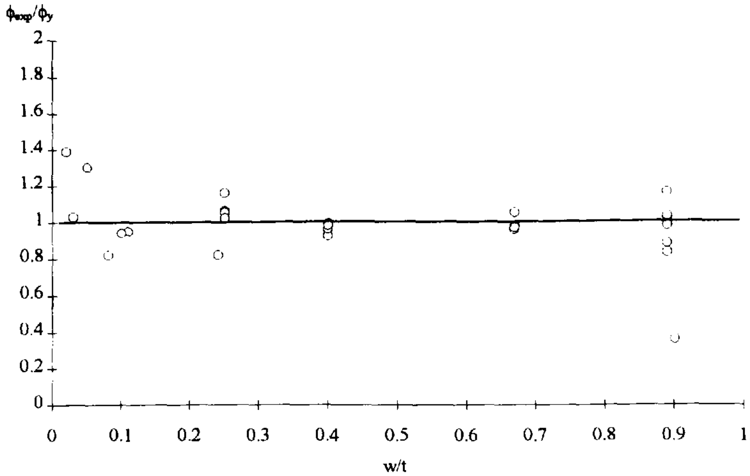

Fig. 7. Strength modelling factor as a function of the level of initial imperfections, w, normalised by the plate thickness, t.

TABLE 3
Ultimate Transverse Compression Strength of Plates with a Slenderness $\beta = 3.51$ ($b/t = 89$) for Two Different Boundary Conditions and Ratio of ϕ_{exp} with the Theoretical Predictions of eqn (6), ϕ_y

α	ϕ_{exp}		ϕ_{exp}/ϕ_y	
	Restr.	*Unrestr.*	*Restr.*	*Unrestr.*
2	0.38	0.30	1.03	0.83
3	0.26	0.22	1.02	0.88
5	0.16	0.15	1.03	0.98

$$B_c = 0.7 + 0.05\alpha. \tag{18}$$

Finally, it is worth mentioning that a wide plate is considered to have, in general, an aspect ratio α at least larger than 2. In fact, this was the basis used to derive the equations discussed in this section.

For plates with $1 \leq \alpha \leq 2$ the mode of collapse assumed for transverse compression strength modelling is no longer valid, i.e. the separation of the plate into a central region and into two others adjacent to the edges becomes less applicable. In these situations one could use the results derived by Guedes Soares and Faulkner[12] for the uniaxial longitudinal compression strength of plates with $0.5 \leq \alpha \leq 1$. These formulations [eqns (9)–(11)] would correspond to the transverse strength of plates with $1 \leq \alpha \leq 2$.

The results of applying eqns (9) and (11) to the set of experiments and numerical data used before is summarised in Table 4. They indicate that the difference in bias between the two formulations is very small, but the data set is too small to allow definite conclusions to be drawn for this range of aspect ratios.

The design formulae proposed in eqns (15)–(18) were derived from calibrations with available numerical and experimental results.

TABLE 4

Comparison of the Predictions of eqns (9)–(11) (GS,F) with other Design Methods

References	β_y	α	*b/t*	*Meas.* ϕ_{exp}	*ABS* ϕ_{exp}/ϕ_y	*Faulk.* ϕ_{exp}/ϕ_y	*Valsg.* ϕ_{exp}/ϕ_y	*GS,G* ϕ_{exp}/ϕ_y	*GS,F* ϕ_{exp}/ϕ_y
Valsgard[15]	0.99	1	25	1.05	1.12	0.98	1.05	1.16	1.05
	1.58	1	40	0.86	1.04	0.76	1.00	0.99	1.00
	1.98	2	25	0.68	0.82	0.68	1.02	1.06	0.81
	2.63	1	67	0.77	1.49	1.02	1.26	1.05	1.26
	2.96	3	25	0.60	0.76	0.61	1.08	1.05	1.01
	3.16	2	40	0.49	0.87	0.65	0.95	0.92	0.89
All numerical S.D.	2.22 0.77	1.7 0.8	37 15	0.74 0.18	1.02 0.24	0.78 0.16	1.06 0.10	1.04 0.07	1.00 0.14
Bradfield[16]	1.56	2.5	15	1.00	1.09	1.39	1.00	1.03	0.98
Bradfield[16]	1.56	1.67	23	0.97	1.00	0.97	1.30	1.39	0.99
Bradfield[16]	1.72	1	38	0.70	0.88	0.65	0.85	0.82	0.85
Bradfield[16]	1.72	1	38	0.74	0.93	0.69	0.90	0.87	0.90
Bradfield[16]	2.48	2.5	24	0.77	0.96	0.78	1.29	1.30	1.09
Bradfield[16]	2.48	1	59	0.62	1.07	0.77	0.96	0.82	0.96
Becker[8]	2.61	1.5	30	0.65	1.08	0.80	1.09	1.04	1.00
Bradfield[16]	2.85	1.67	25	0.55	0.98	0.71	0.99	0.95	0.91
Bradfield[16]	2.85	1.67	35	0.56	1.00	0.73	1.02	0.98	0.94
Becker[13]	3.30	3	30	0.68	0.93	0.76	1.33	1.30	1.30
All experiments S.D.	2.31 0.59	1.8 0.7	33 11	0.72 0.15	1.01 0.16	0.83 0.20	1.07 0.17	1.05 0.20	0.99 0.12
All plates S.D.	2.28 0.67	1.72 0.70	34 13	0.73 0.16	1.01 0.16	0.81 0.19	1.07 0.14	1.05 0.16	0.99 0.13

4 ASSESSMENT OF THE PERFORMANCE OF THE PROPOSED APPROACH

The equations proposed here to evaluate the transverse compression strength of rectangular plates [eqns (15) and (16)] were derived from existing experimental and numerical results which did not necessarily cover the complete range of slendernesses and aspect ratios. Therefore, in order to test the performance of the formulation proposed in this work over the full range of slendernesses and aspect ratios, the strength of a series of plates was computed using a finite element program, which accounts for large deflections, elasto-plastic behaviour and initial imperfections.[17]

The range of plate slenderness covered lies between 0.85 and 4.23, and the aspect ratio of the plates between 2 and 5. The initial imperfections were chosen in such a way that the real collapse mode of the plate is coincident with the lowest collapse mode (single half-wave). Their amplitudes are *ca* $0.1\beta^2 t$, but all of the plates have more than one sinusoidal component in order to have more realistic models without symmetry. The boundary conditions are simply supported for all plates and the edges are forced to remain straight. The 'unloaded' edges have no in-plane displacement during the loading which corresponds to the restrained conditions. In these series of calculations residual stresses were not imposed.

Table 5 summarises the main geometric parameters of the plates, the initial imperfections and the corresponding transverse strength. Comparisons with the proposed formula are given.

The most general conclusion is the confirmation that the results obtained with finite element codes tend to predict higher values than those obtained in experimental tests. The average of the normalised strength is very close to 1.0 and the coefficient of variation, COV, is 11%, which is a good value considering that the effect of distortions it not explicitly accounted for in the proposed design equations.

A more detailed analysis shows that this approximate formula predicts the transverse strength of plates very well, especially at high aspect ratios. Stocky plate strength prediction tends to be conservative. Intermediate slenderness plates with low aspect ratio ($\alpha < 3$) have their strengths over estimated (Fig. 8).

Another important feature of the plate behaviour under transverse loading is that stocky plates collapse at much lower strains than slender ones. The ultimate strain tends to increase with the slenderness but remains close to 1 when the slenderness is lower than 1.8. For slendernesses higher than 2.8 the ultimate strain is always higher than 1.5 times the yield strain and no evidence of load shedding after buckling may be detected, while for stocky plates the decrease in the post-buckling strength is always present (Fig. 9). Also, the

TABLE 5
Compression Strength of Transversely Loaded Plates Predicted by a Non-linear Finite Element Code, and Compared with the Design Equation Predictions

α	β	$w_{max}/(t\beta^2)$	ϵ_u/ϵ_0	ϕ_{cal}	ϕ_y	ϕ_{cal}/ϕ_y
2	0.85	0.154	0.971	0.861	0.688	1.251
2	1.69	0.075	1.067	0.509	0.510	0.998
2	2.82	0.092	1.519	0.356	0.401	0.889
2	3.38	0.077	1.568	0.329	0.370	0.891
2	4.23	0.062	1.601	0.304	0.337	0.901
2.5	0.85	0.134	0.938	0.804	0.660	1.217
2.5	1.69	0.101	1.119	0.439	0.441	0.995
2.5	2.82	0.080	1.610	0.301	0.335	0.897
2.5	3.38	0.084	1.553	0.271	0.306	0.887
2.5	4.23	0.081	1.588	0.246	0.275	0.894
3	0.85	0.114	0.915	0.767	0.648	1.184
3	1.69	0.129	1.026	0.416	0.396	1.052
3	2.82	0.103	2.428	0.262	0.290	0.901
3	3.38	0.086	2.540	0.241	0.261	0.921
3	4.23	0.098	2.730	0.217	0.232	0.935
4	0.85	0.113	0.876	0.738	0.643	1.146
4	1.69	0.098	1.064	0.358	0.339	1.056
4	2.82	0.078	1.557	0.219	0.231	0.946
4	3.38	0.081	1.584	0.191	0.203	0.942
4	4.23	0.078	1.545	0.165	0.172	0.956
5	0.85	0.122	0.818	0.718	0.654	1.098
5	1.69	0.105	1.027	0.330	0.307	1.076
5	2.82	0.084	1.500	0.194	0.193	1.005
5	3.38	0.088	1.570	0.166	0.163	1.014
5	4.23	0.084	1.515	0.142	0.131	1.082

tangent modulus is very different for these two slendernesses and even at the very beginning of the load shortening curve the tangent modulus is much lower than the Young's modulus of the material in the case of the plate with $\beta = 4.23$.

The sensitivity of the formulation with the aspect ratio is low (Table 6) and the spread of the results, ϕ_{cal}/ϕ_y, tends to reduce as α increases. Note that a COV of 4% with $\alpha = 5$ is a very good result, especially as the COV tends to increase drastically at very high aspect ratios.

For $\alpha = 2$ and 2.5, it should be noted that in spite of the calculated results being greater than the predictions on average, the average of the normalised results is lower than unity. This is due to the very low predictions at low slenderness for these aspect ratios (Fig. 8).

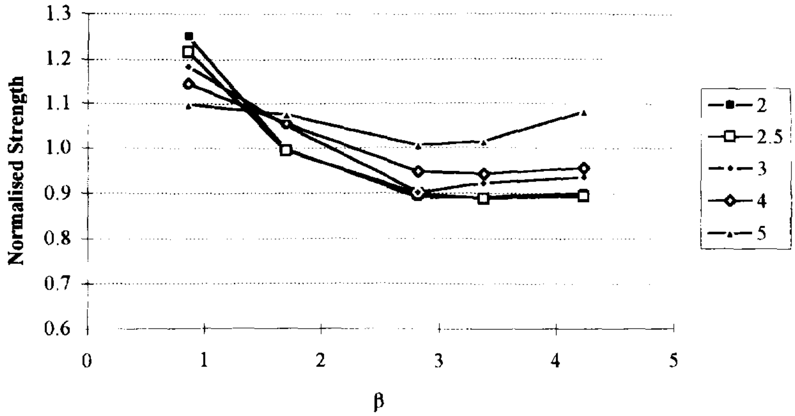

Fig. 8. Summary of the transverse strength of plates calculated by the finite element code and normalised by the strength given by eqns (15) and (16b).

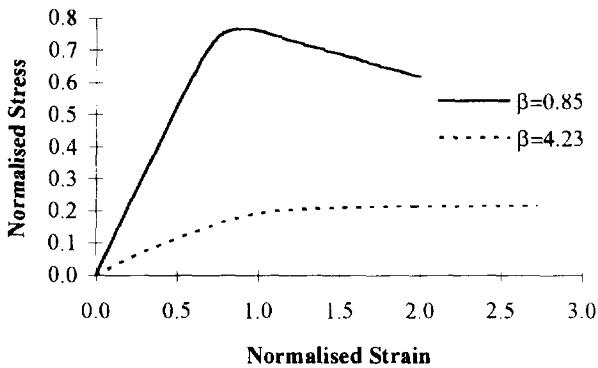

Fig. 9. Average transverse stress–average strain of plates of aspect ratio 3 with transverse loading and restrained edges.

TABLE 6

Summary of the Average Strength of Transversely Loaded Plates and Comparison with the Design Equation Predictions for each Aspect Ratio

a/b	*Avg* ϕ_{cal}	*Avg* ϕ_{y}	*Avg* ϕ_{cal}/ϕ_{y}	*COV* ϕ_{cal}/ϕ_{y}
2	0.472	0.461	0.979	0.143
2.5	0.412	0.403	0.978	0.144
3	0.381	0.365	0.999	0.119
4	0.334	0.318	1.009	0.089
5	0.310	0.290	1.055	0.040
All	0.382	0.367	1.005	0.109

5 CONCLUDING REMARKS

The transverse compression strength of plate elements is assessed on the basis of data collected from tests and numerical results. Comparisons with the predicted strength from several formulations are performed and based on these results an alternative formula for transverse strength prediction is proposed. Because of the qualitative differences between tests and numerical results, especially for high plate slendernesses, the new formulation was derived based on the numerical results. The reduction factor due to unrestrained unloaded edges is also computed.

The proposed design equations [(15) and (16)] have been verified for a series of plates, covering a wide range of aspect ratios and plate slendernesses, whose transverse strength was determined from calculations performed with a non-linear finite element code.

ACKNOWLEDGEMENT

This research work was performed under a research contract with the American Bureau of Shipping to whom the authors express their appreciation.

REFERENCES

1. Guedes Soares, C., Probabilistic analysis of flat compression members, *Proc. of Advanced Seminar on Structural Reliability*, CEC Joint Research Centre, ISPRA Establishment, Italy. 11–15 May, 1989.
2. Guedes Soares, C., Design equation for the compressive strength of unstiffened plate elements with initial imperfections. *J. Construct. Steel Res.*, **9** (1988) 287–310.
3. Bleich, F., *Buckling Strength of Metal Structures*, McGraw-Hill, New York, 1952.
4. Carlsen, C. A., *Collapse of Stiffened Panels in Compression. Rep 1: Plate Between Stiffeners*, Report No. 76-306, 1976, Det Norske Veritas.
5. Schultz, H. G., Über die effektive Breite Druckbeanspruchter Schiffsplatten und das effektive Widerstandsmoment des Schiffskastenträngers mit Ausbeulendem Längsverband. *Schiff und Hafen*, **8** (1964).
6. Blanc, F., Discussion of ultimate longitudinal strength. *Trans. RINA*, **107** (1965) 426–430.
7. Faulkner, D., Adamchak, J. C., Snyder, G. J. & Vetter, M. F., Synthesis of welded grillages to withstand compression and normal loads. *Computers and Structures*, **3** (1973) 221–246.
8. Becker, H. & Colao, A., *Compressive Strength of Ship Hull Girders. Part III. Theory and Additional Experiments*, Report SSC-267. Ship Structure Committee, Washington D.C., 1977.

9. Becker, H., Instability strength of poliaxially-loaded plates and relation to design. *Steel Plated Structures*, ed. P. J. Dowling *et al.*, Crosby, Lockwood and Staples, London, 1977, pp. 559–580.
10. Valsgard, S., *Ultimate Capacity of Plates in Transverse Compression*, Report 79-104, Det Norske Veritas, 1979.
11. Faulkner, D., A review of effective plating for use in the analysis of stiffened plating in bending and compression. *J. Ship Res.*, **19** (1975) 1–17.
12. Guedes Soares, C. & Faulkner, D., Probabilistic modelling of the effect of initial imperfections on the compressive strength of rectangular plates, *Proc. of Third International Symposium on Practical Design of Ships and Mobile Units (PRADS)*, Trondheim, Vol. 2, 1987, pp. 783–795.
13. Becker, H., *et al., Compressive Strength of Ship Hull Girders. Part I. Unstiffened Plates.* Report SSC-217. Ship Structure Committee, Washington D.C., 1970.
14. Dowling, P. J., Harding, J. E. & Slatford, J. E., *Plates in Biaxial Compression—Final Report*, CESLIC Report SP4, Dep. Civil Engng, Imperial College of Science and Technology, 1979.
15. Valsgard, S., Numerical design prediction of the capacity of plates in in-plane compression. *Computers and Structures*, **12** (1980) 729–739.
16. Bradfield, C. D. & Porter Goff, R. F. D., *Compressive Tests on Steel Plates of Low Aspect Ratio*, Report CUED/C-Struct/TR48, Cambridge University, Engineering Department, 1975.
17. Kmiecik, M., The influence of imperfections on the load carrying capacity of plates under uniaxial compression. *Ship Technol. Res.*, **39** (1992) 17–27.